



# Electrochemical corrosion of a glassy carbon electrode

Youngmi Yi<sup>a</sup>, Gisela Weinberg<sup>b</sup>, Marina Prenzel<sup>a</sup>, Mark Greiner<sup>a,b</sup>, Saskia Heumann<sup>a,\*</sup>,  
Sylvia Becker<sup>a</sup>, Robert Schlögl<sup>a,b</sup>

<sup>a</sup> Max Planck Institute for Chemical Energy Conversion, Stiftstrasse 34-36, 45470 Mülheim an der Ruhr, Germany

<sup>b</sup> Fritz Haber Institute of the Max Planck Society, Faradayweg 4-6, 14195 Berlin, Germany

## ARTICLE INFO

### Keywords:

Carbon corrosion  
Carbon electrode  
Glassy carbon  
Electrochemical oxidation  
Acid catalyzed addition/substitution  
Radical substitution  
Local selective oxidation

## ABSTRACT

Glassy carbon is widely used in electrochemistry due to its properties of high temperature resistance, hardness, low density and low electrical resistance. The present study focuses on the chemical resistance under electrochemical oxidative conditions, which occur under oxygen-involving reactions like oxygen reduction reaction (ORR) and oxygen evolution reaction (OER). The electrochemical performance of glassy carbon investigated in alkaline, neutral and acidic media reveal the same chemical processes during the OER but showing different degradation mechanism.

The electrochemical signature of the corrosion in different media could be directly associated with the formation of oxygen functional groups determined by spectroscopic methods like Raman, infrared (IR) and x-ray photoelectron spectroscopy (XPS). The morphology change of the carbon surface caused by carbon oxidation was investigated by microscopy. A rough surface was obtained in the acidic case, whereas dents were seen in alkaline media.

It is assumed that the glassy carbon electrode in acidic media degrades by forming surface oxides by acid catalyzed process leading to ring opening in the graphitic structure and therefore oxidation in the bulk. In alkaline media OH radicals preferentially react with alkyl site chains, leading to oxidation of the edges of carbon layers until they become hydrophilic and dissolve.

## 1. Introduction

A variety of nanostructured carbon materials, such as carbon nanotube, mesoporous carbon and graphene, have been utilized in heterogeneous catalyst and electrocatalysis for a catalyst support to improve the catalytic efficiency due to the better catalyst utilization and reduction of the catalyst loadings. At a point of booming interest in metal-free catalysts for electrochemical reactions, carbon materials have been applied itself as electrocatalyst. One of the well-known approaches is oxygen reduction reaction (ORR) on nanostructured carbon materials. Extensive studies have reported that nitrogen-containing carbon materials possess similar catalytic activity for ORR in alkaline media as a commercial carbon supported Pt catalyst [1–4]. Very recently, carbon materials were used as electrocatalysts for water oxidation, which is the oxygen evolution reaction (OER), in spite of carbon corrosion at oxidative conditions. The selected literatures about OER on carbon electrodes are listed in Table S1. Carbon doped with heteroatoms [5], [6,7] or surface-oxidized carbon [8,9] show good electrochemical performance for OER that is even comparable to metal(oxide) catalysts. Furthermore, many efforts are under way to identify the

catalytic sites for ORR and OER on carbon materials by analyzing the surface change of carbon electrodes before and after the reaction [5,10]. Although the electrocatalytic activity of carbon materials could be used potentially as metal-free catalysts, the instability of carbon materials at its condition are rarely considered. Because the standard potential of carbon oxidation reactions is 0.207 V vs. RHE [11], carbon corrosion is inevitable at high anodic potential. At the cathode of fuel cells, where ORR takes place, the potential goes up to 1.4 V in abnormal conditions due to fuel starvation [12,13]. At the anode of electrolyzers, where OER occurs, the operating potential for the OER is practically above 1.5 V [14–16]. Under these anodic conditions, the oxidation of carbon to CO<sub>2</sub> and/or CO leads to the destruction of the carbon electrode.

Beyond many studies on ORR and OER activity of carbon-based catalysts, we intend to investigate the change of carbon electrodes due to its instability at oxidative conditions. In our previous study [17], we investigated the electrochemical degradation of multiwall carbon nanotubes (MWCNTs) in acidic media. MWCNTs at high anodic potential for OER in acidic media undergo first electrochemical activation by forming functional groups, followed by a passivation due to a fully

\* Corresponding author.

E-mail address: [saskia.heumann@cec.mpg.de](mailto:saskia.heumann@cec.mpg.de) (S. Heumann).

<http://dx.doi.org/10.1016/j.cattod.2017.07.013>

Received 13 February 2017; Received in revised form 4 July 2017; Accepted 10 July 2017

Available online 12 July 2017

0920-5861/ © 2017 The Authors. Published by Elsevier B.V. This is an open access article under the CC BY license (<http://creativecommons.org/licenses/by/4.0/>).

covering oxide layer. In the present work, we chose glassy carbon as the investigating material, and compare the corrosion behavior of a carbon depending on the pH of electrolyte.

Glassy carbon (GC) is a type of non-graphitic carbon formed by pyrolysis of certain polymeric precursor. The microstructure of GC is composed of discrete fragments of curved carbon planes, like imperfect fullerene-related nanoparticles. GC synthesized at high temperatures above 2000 °C exhibits a network of stacked graphite-like ribbon molecules. Entities of polyhedral graphite crystals were also detected in commercial glassy carbon as used in our studies [18]. The network of randomly and tangled carbon planes forms a dense carbon structure. Due to low reactivity, high hardness, impermeability and good electrical conductivity of GC, it is commonly employed as an electrode material for electroanalysis [19,20]. Due to the assumed chemical inertness, it is also often used as a substrate to cast powder catalysts in order to evaluate their catalytic performance in electrochemical reactions. However, at high anodic potentials carbon oxidation can occur, giving rise to deterioration of the electrode and potentially affecting the evaluation of the electrochemical performance of catalysts. Nevertheless electrochemical oxidation of carbon can be advantageous for electrochemical sensors, as it is generally agreed that the electrochemical oxidation of GC activates the electrode surface, leading to faster electron transfer kinetics [21–24].

The results demonstrated in the present study are important for interpreting electroanalytical and electrocatalytic data from studies using GC electrodes. We investigated the morphology and surface change of carbon electrodes caused by prolonged oxidation at high anodic potentials. To consider the wide variety of environments experienced in electrocatalytic reactions, the electrochemical degradation of carbon electrodes was characterized depending on the pH, especially acidic, neutral and alkaline media. The different degradation behavior of the carbon electrodes, and its dependence on the pH of electrolyte, is documented in this study. Since carbon is commonly used as an electrode material for electroanalytical and catalytic applications, the understanding of the electrochemical stability of carbon electrodes is of crucial importance for the electrochemical community.

## 2. Experimental

Glassy carbon (GC) disks (SIGRADUR G discs, 1 mm thick and 10 mm diameter, polished with diamond  $R_a > 50$  nm) were purchased from HTW (Hochtemperatur-Werkstoffe GmbH, Germany).

The electrochemical experiments were performed using a standard three-electrode cell consisting of a Pt wire as a counter electrode, a standard calomel electrode (SCE) and a mercury/mercury oxide (Hg/HgO) reference electrode. All values of the potential were corrected to reversible hydrogen electrode (RHE) [25]. The electrochemical oxidation of GC was performed in 0.5 M  $H_2SO_4$ , 0.5 M  $K_2SO_4$ , or 0.1 M KOH at the applied potential of 1.8 V vs. RHE for 24 h under Ar bubbling. In order to analyze the electrochemical change of the GC electrode, cyclic voltammetry was carried out in a range of potentials between the oxygen and hydrogen evolution reactions.

The GC before and after the prolonged electrochemical oxidation were characterized with several techniques to examine the change in morphological and physicochemical properties upon oxidation. The morphological changes of GC were determined by scanning electron microscopy (SEM, Hitachi) and atomic force microscopy (AFM). Energy-dispersive X-ray spectroscopy (EDX) was conducted, in conjunction with the SEM analysis, to analyze the elemental composition of the carbon surface. Raman spectroscopy was performed on a Thermo Scientific DXR Raman Microscope with a  $50\times$  magnification and 532 nm laser. Infrared spectroscopy was carried out in the attenuated total reflection (ATR) mode (Thermo Scientific Nicolet iS50) using a DTGS detector and a diamond crystal. X-ray photoelectron spectroscopy (XPS) was measured using a Versaprobe spectrometer from Physical Electronics (PHI 5000 VersaProbe) employing monochromatic Al K $\alpha$

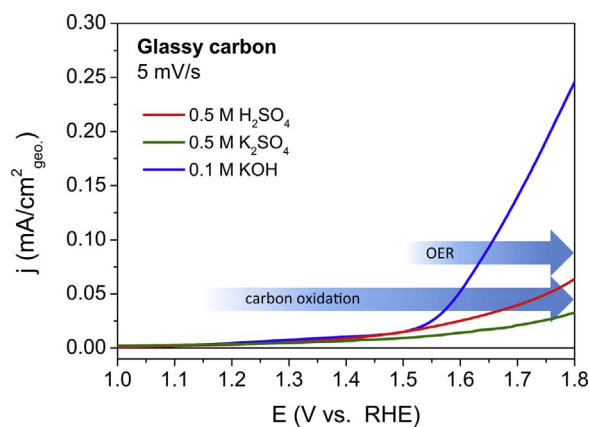


Fig. 1. Linear sweep voltammetry of GC disc at high anodic potential in 0.5 M  $H_2SO_4$  (acidic), 0.5 M  $K_2SO_4$  (neutral) and 0.1 M KOH (alkaline). Scan rate: 5 mV/s.

(1486.6 eV) radiation with a spectral resolution of 0.35 eV at pass energy of 23.5 eV. All measurements were performed with a spot size of 200  $\mu$ m diameter and with a take-off angle for 45°. The binding energy scale of the system was calibrated using clean gold surface with Au4f $_{7/2}$  at 83.98 eV, and correction using the C1s peak and valence band spectrum resulted in a constant position of the C1s core level at 284.5 eV  $\pm$  0.2 eV.

## 3. Results and discussion

Linear sweep voltammograms (LSV) of GC are shown in Fig. 1, scanned at anodic potentials between 1.0 and 1.8 V in acidic, neutral and alkaline media. The thermodynamic potential for carbon and water oxidation is at 0.207 V and 1.23 V vs. RHE, respectively. Because of slow reaction kinetics and intrinsic properties of the electrode materials, these reactions generally start above the thermodynamic potential. The oxidation current of GC gradually rises with sweeping of the anodic potential, where two notable points can be observed. At around 1.2 V a slight increase of the current is observable which can be mainly attributed to carbon oxidation. Above 1.5 V vs. RHE a significant increase of current is detected due to the anodic oxidation of water (OER) and ongoing carbon oxidation.

The electrochemical oxidation process on a carbon electrode is influenced by the water oxidation and can be confirmed by chronoamperometric measurements of GC applied at oxidative potentials in acidic media. The transient anodic current on a GC electrode at a fixed potential of 1.2 and 1.5 V gradually declines to a steady-state value (Fig. S1). Once oxygen evolution caused by water oxidation is involved in the oxidation process on the carbon electrode, at an applied potential of 1.8 V, the initial current increases with time, assuming that the surface of the carbon electrode undergoes vigorous change due to the oxidation. In order to investigate the surface change of GC caused by carbon oxidation, it was subjected to prolonged electrolysis at an anodic potential of 1.8 V vs. RHE where both, water and carbon oxidation, occurs simultaneously. Fig. 2 shows the chronoamperometry of GC at the anodic potential in 0.5 M  $H_2SO_4$  (acidic), 0.5 M  $K_2SO_4$  (neutral) and 0.1 M KOH (alkaline) solution. Significant current peaks are observed in the different media, which can be related to the formation of oxygen species on the GC electrode. The oxidation process is most rapidly in alkaline media, followed by the oxidation in acidic media. A steady state and therefore steady current is reached after one hour in both cases. The transition of oxidation current in neutral media is much lower and slower than in the other media, indicative of slow kinetics of the oxidation. A close look at Fig. 1 (Fig. S2) supports these observations also on the short time scale as the current increase assigned to the oxidation process begins at 1.2 V in alkaline media, at slightly higher potential in acidic media and convoluted to determine

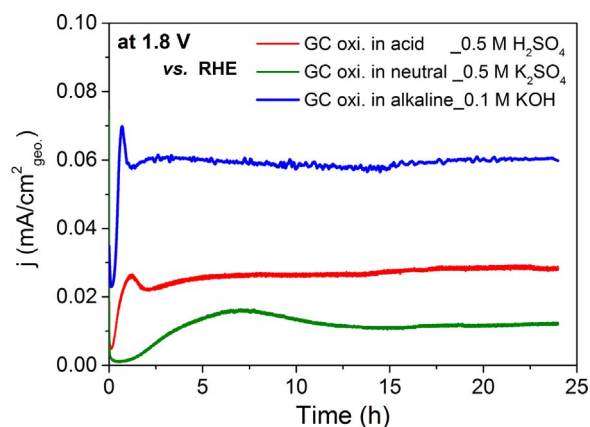


Fig. 2. Chronoamperometry on glassy carbon (GC) applied at 1.8 V vs. RHE with different pH media.

exactly at even higher potentials in neutral media. Increasing the oxidation current at anodic potentials means that the carbon electrode undergoes an activation with respect to the electrochemical reactions [17,21,23]. After initial changes, the current on GC remains almost constant during the oxidation, indicating that the oxidation current stabilizes with the prolonged oxidation. Even though the oxidation current in acidic media is lower than alkaline media, the oxidation current profile follows the same trend in all different pH environments.

The cyclic voltammograms (CV) of the GC electrode recorded at a potential between the hydrogen and oxygen evolution reaction are shown in Fig. 3. The charge of CV in this range can determine the electrochemical capacitance. The electrochemical oxidation of the GC leads to the formation of a porous and hydrated surface layer, corresponding to increased capacitance [11,26,27]. The magnitude of the current in the cyclic voltammogram of GC that was oxidized in acidic media increases considerably with the oxidation time, as seen in Fig. 3(a). Furthermore, the redox peak around 0.55 V vs. RHE becomes more pronounced as the carbon becomes more oxidized. These observed faradaic current peaks can be attributed to surface functional groups which are electrochemically active [28,29], suggesting that surface oxides are formed on carbon surface during the oxidation in acidic media. In comparison with the oxidation behavior in acidic media, the electrochemical capacitance in neutral and alkaline media during the oxidation increases without the pronounced faradaic peaks. The change of the electrochemical capacitance calculated by integrating the CV curves is displayed in Fig. 3(b), (d) and (f). The electrochemical capacitance of GC increases rapidly in the beginning followed by a linear increase with time in acidic media, indicating an ongoing oxidation process that might be coupled with an increase of surface area. The capacitance of the GC electrode after 24 h of oxidation at 1.8 V is almost 300 times larger than that of pristine glassy carbon in acidic media. The increase of capacitance in alkaline media is very rapid until it reaches a plateau around 0.5 mF within one hour, implying a balanced equilibrium. The slight increase in capacity on the plateau can be explained by the constant increase of the surface area due to leaching effects of the carbon as explained later. Therefore, because of changing specific surface areas over time during electrochemical oxidation the absolute values of the capacity are shown instead of geometric area related capacities. The progress of the capacitance in neutral media shows similar behavior as acidic media, but is slow in comparison to other media.

Denkanski *et al.* [30] have previously reported on the change of capacitance during electrochemical oxidation of glassy carbon in acidic and alkaline media. They found that the decrease of CV on oxidized GC in acidic media is due to the peeling off of a carbon oxide layer, as apparent by the visible color change of the electrolyte to yellow-brown with polarization time. Compared to the oxidation conditions applied

by Denkanski *et al.*, our conditions are mild, with an applied potential always less than 2 V vs. RHE. Thus, the stage of full destruction of the carbon oxide film had not yet been reached. In contrast to our conditions in alkaline KOH, the electrolyte turns to a brown-colored solution during the electrochemical oxidation of carbon (Fig. S3). The substance responsible for the brown color is likely to be either carbon nanoflakes and/or soluble organic compounds that were leached out during corrosion of the carbon electrode in alkaline media [11,31]. The brown-colored solution was measured in UV/Vis adsorption to identify the brownish substance in the KOH electrolyte (Fig. S5). An intense peak at around 220 with the slight shoulder at 235 nm was observed in the spectra of the KOH solution after the electrochemical oxidation of carbon. The peaks at 220–300 nm represent a typical absorption of polycyclic aromatic hydrocarbons. In addition, the UV–vis spectrum of the brownish substance is similar to carbon dots which are small carbon nanoparticles less than 10 nm in size. This points to dissolved carbon fragments from the carbon electrode caused by carbon oxidation, which could be also related to the exfoliation of carbon.

In order to understand the changes that occur to the GC electrode surface during prolonged electrolysis at an anodic potential, morphological and structural analysis of pristine GC and GC, oxidized in acidic, neutral and alkaline media, were performed.

The SEM images shown in Fig. 4 reveal the morphological changes to the GC surface caused by oxidation in different media. The surface of pristine GC is smooth and flat (Fig. 4(a)). Electrochemical oxidation leads to the destruction of carbon surface. Thus, the rough and porous surface of the GC samples was observed after the prolonged oxidation. Furthermore, depending on the pH of the electrolyte during oxidation, the surface of GC exhibits different morphologies. For the GC oxidized in acidic media, it seems that an oxide layer was grown on the carbon surface caused by the oxidation (Fig. 4(b)). The carbon surface of the GC oxidized in neutral media looks similar to acidic media, but the domains are larger and the surface looks more bumpy and dimply than in acidic media. On the other hand, the GC oxidized in alkaline media exhibits several dents with various forms (Fig. 4(d)). More SEM images were collected in Fig. S6 to support these observations. The dents are presumably formed via carbon dissolution in alkaline media revealing an unoxidized carbon surface as observed before in Fig. 3. The CV of GC electrode increases without the appearance of faradaic current peaks, which correspond to surface oxides. Thus, the increase of GC surface area caused by the carbon dissolution in alkaline media can explain the influence on the increasing electrochemical capacitance on the GC during the electrochemical oxidation in alkaline media. As described earlier, additional evidence for carbon dissolution is the brown coloration of KOH electrolyte after the oxidation. Furthermore, we observed a difference in the GC mass before and after the electrochemical oxidation, with oxidation giving rise to a 0.3% decrease in mass (Fig. S2). In contrast, no measurable mass change was found for GC oxidized in acidic media.

The elemental analysis of the oxidized carbon electrode measured by EDX coupled with SEM supports the different corrosion behavior in acidic and alkaline media. The GC oxidized in acidic media exhibits a significant increase of oxygen signal compared the pristine GC, shown in Fig. S4 and Table 1. Additionally, we could detect a small amount of sulfur from the electrolyte, H<sub>2</sub>SO<sub>4</sub>. In contrast, there is no obvious change in the elemental composition on the pristine and the GC oxidized in alkaline media. These observations are a clear evidence for the formation of oxides during the oxidation process. The previous study in Kötz *et al.* [27,32,33] also observed the growth of an oxide film on carbon electrodes oxidized in acidic media with AFM and Ellipsometry. Therefore, it can be concluded that the glassy carbon electrode is oxidized by forming oxides in acidic media, while in alkaline media carbon oxidation leads to carbon dissolution during the oxidation process.

Atomic force microscopy (AFM) images give additional information about the morphological changes that accompany electrochemical oxidation, as shown in Fig. S7. These result are in line with

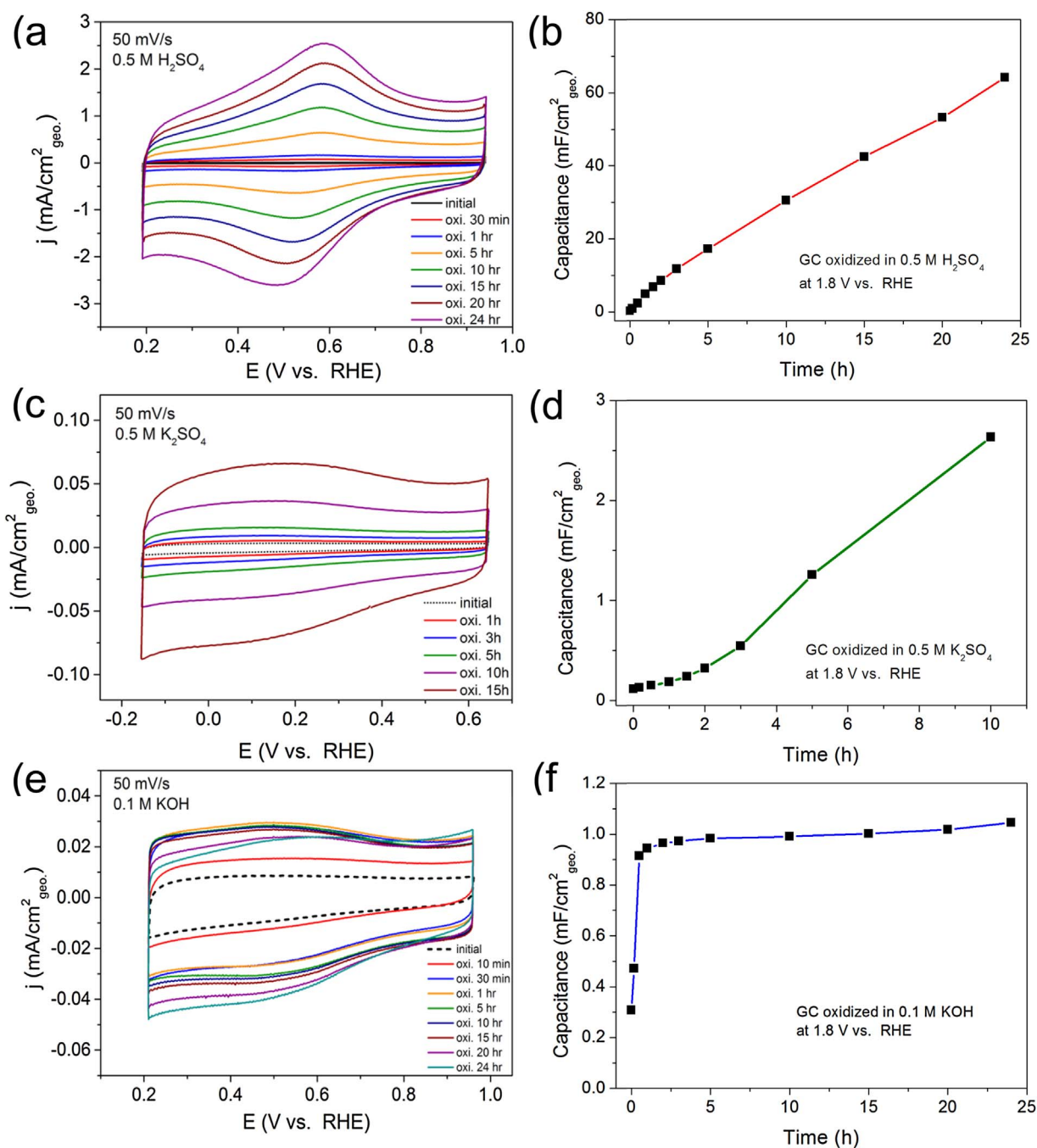


**Fig. 3.** Cyclic voltammetry (CV) of GC during the electrochemical corrosion in acidic (a), neutral (c), and alkaline (e) media. The change of electrochemical capacitance determined from CV curves (b), (d), and (f).

morphological features seen in SEM. The smooth surface of the pristine GC becomes roughened with electrochemical oxidation. The GC oxidized in acidic media contains a few flakes on the surface, probably the evidence of carbon oxide grown on the surface. This finding supports the observation of the previous AFM study by Kötter et al. They prove the significant volume increase on the activated region of carbon surface during the growth of oxide film, caused by the oxidation in acidic media. In contrast, the surface morphology of the GC oxidized in alkaline media reveals the macroscopic degradation by carbon dissolution. The roughness of the GC surfaces increases due to the carbon oxidation, with a roughness of 15 Å for pristine GC, 38 Å for GC oxidized in acidic media, and 87 Å for GC oxidized alkaline media. While the surface oxides formed on GC in acidic media, the roughness increased by a factor of 2.5, the dissolution of GC in alkaline media

forms dents that increase the roughness more intense by a factor of 5.8.

The structural and chemical changes of the GC electrode by oxidation were confirmed by Raman and infrared spectroscopy. Fig. 5(a) shows the Raman spectrum of the GC electrodes. The spectrum of the oxidized GC in alkaline media is almost identical to the spectrum of polished GC. It can be assumed that significant change on graphite crystallite occurs during the carbon oxidation at low pH. Raman spectra of GC samples have three dominant bands at ca. 1360 cm<sup>-1</sup> (defect, D band), 1620 cm<sup>-1</sup> and at ca. 1580 cm<sup>-1</sup> (graphitic, G band) caused by resonant phonon vibrations of the graphitic structures. In general, D, D' and G bands were used to determine the degree of disorder in carbons [34,35]. The ostensible increase of the intensity of the G band was observed on the GC oxidized at low and neutral pH. This change of G band in non-graphitic carbon does not arise from phonon vibrations by



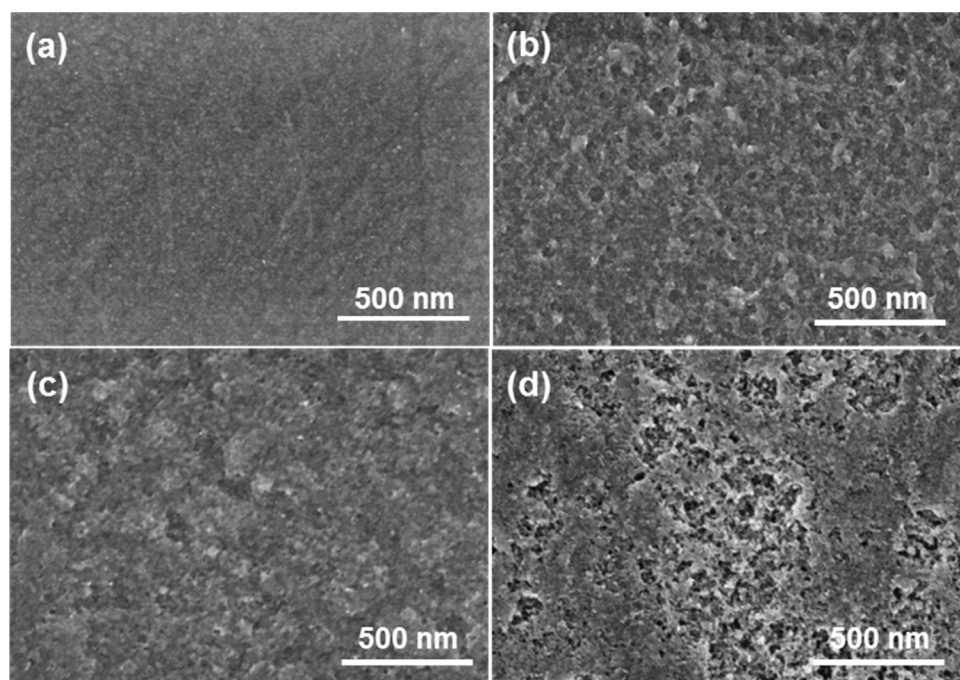


Fig. 4. SEM images of pristine GC (a), GC oxidized in acidic (b), neutral (c), and alkaline (d) media operated at 1.5 kV with secondary electron.

**Table 1**  
Elemental composition as determined by SEM-EDX and XPS.

	Determined by SEM-EDX		Determined by XPS	
	C at. %	O at. %	C at. %	O at. %
Pristine GC	99.24	0.76	90.88	9.12
GC oxidized in acid	85.66	14.17	79.54	20.46
GC oxidized in alkaline	99.43	0.57	80.53	19.47

a higher degree of graphitization, but rather results from the effect of molecular vibrations in the spectra. In non-graphitic carbon with large amounts of defects, the G band retains its intensity and D/G ratio decreases with increasing amorphisation [36,37]. Moreover, the intensity at ca.  $1500\text{ cm}^{-1}$  between the D and G bands originates from amorphous carbon entities, such as organic molecules, fragments, and non-graphitic carbon with a high density of functional groups and/or defects [35,38]. At low pH of electrolyte during carbon oxidation, the band intensity at ca.  $1500\text{ cm}^{-1}$  increases significantly. This indicates, that the carbon electrode oxidized at low pH, contains the aforementioned entities. This information on amorphous phases originates from oxide species formed by carbon oxidation, consistent with SEM and AFM analysis discussed above. Although the macroscopic destruction of carbon surface was observed in the GC oxidized in alkaline media, no clear evidence of increased edge plane exposure or decrease nominal crystallite size was founded from bulk sensitive Raman spectroscopy.

Chemical information on the termination of the GC electrodes after electrochemical oxidation was obtained from IR spectroscopy, shown in Fig. 5(b). The GC oxidized in acidic media present more pronounced bands than pristine GC. Bands in the region of  $1800\text{--}1400\text{ cm}^{-1}$  can be assigned to carbonyl, carboxyl groups, quinones, and ketones. Especially, the absorption observed at  $1565\text{ cm}^{-1}$  could be ascribed to C=C stretching of polyunsaturated species. Additionally, the absorption band at  $1180\text{ cm}^{-1}$  with the shoulder is corresponding to C–C stretching and –OH bending modes in ether, lactones, carboxyl and phenolic structures [39–41]. The intensities of those bands increase after the oxidation in acidic media. It is evident that surface functional groups are formed during the oxidation of carbon in acidic media. In the GC oxidized in neutral media, small peaks at  $1565\text{ cm}^{-1}$  and around  $1180\text{ cm}^{-1}$  were observed, indicating that less oxidation than in

acidic media occurs. Moreover, the broad band from  $3000$  to  $3600\text{ cm}^{-1}$ , which is associated with the hydroxyl stretching contributions from adsorbed water, is observed in GC oxidized in acidic and neutral media. It is clear that the oxidation in acidic and neutral media induces a hydrophilic surface of GC. On the other hand, the IR spectrum of the GC oxidized in alkaline media is identical with the one of pristine GC. It means that the oxidation of the carbon electrode at high pH produces no oxide species which is detectable on the bulk of the GC. Therefore, the IR results confirm that during the electrochemical oxidation in low pH media surface oxide species are formed.

XPS measurements of GC samples were performed to analyze surface species formed by electrochemical oxidation in detail. The XPS survey spectrum of the surface and subsurface layers on GC electrodes showed the presence of oxygen (O1s) at  $532\text{ eV}$  and carbon (C1s) at  $284\text{ eV}$ . The oxygen content determined by XPS is similar for GC oxidized in both acidic (20.46 at. % O) and alkaline (19.47 at. % O) media, even though an increase of oxygen content was observed only on the GC oxidized in acidic media by SEM-EDX, as listed in Table 1. The difference in oxygen content, determined by the two analysis methods, can be explained by the contrast of surface and bulk sensitivity. It is clear that the change of oxygen content of GC oxidized in alkaline media occurs mainly at the surface or near surface layers.

Since in deconvoluting the C1 s spectrum several extrinsic and intrinsic effects can lead to ambiguous interpretations [42,43], we focus on evaluating the O1 s spectrum. The O1 s signal was fit using 6 peaks, based on the model described in the PhD thesis of Li [44]. The fitting results are shown in Fig. 6, and the integral values of each O1 s peak in the deconvoluted O1 s spectra are listed in Table 2. When pristine GC undergoes prolonged oxidation in acidic media, the C–O of hydroxyl and carboxylic group is mainly present. It is likely that C–O bond types of surface functional groups are responsible for the increase of electrochemical capacitance on the oxidized carbon. In general, the faradaic peak current in cyclic voltammogram of a carbon electrode is known for the redox reaction of quinones which are one of C–O bond functional groups (Eq. (1)) [45,46]. This evidence strongly supports the formation of an oxide layer on the GC during the oxidation in acidic media.

On the other hand, the electrochemical oxidation of carbon in alkaline media mainly leads to an increase of C=O carbonyl compared to other functional groups. Difference O1 s spectra (taken by subtracting

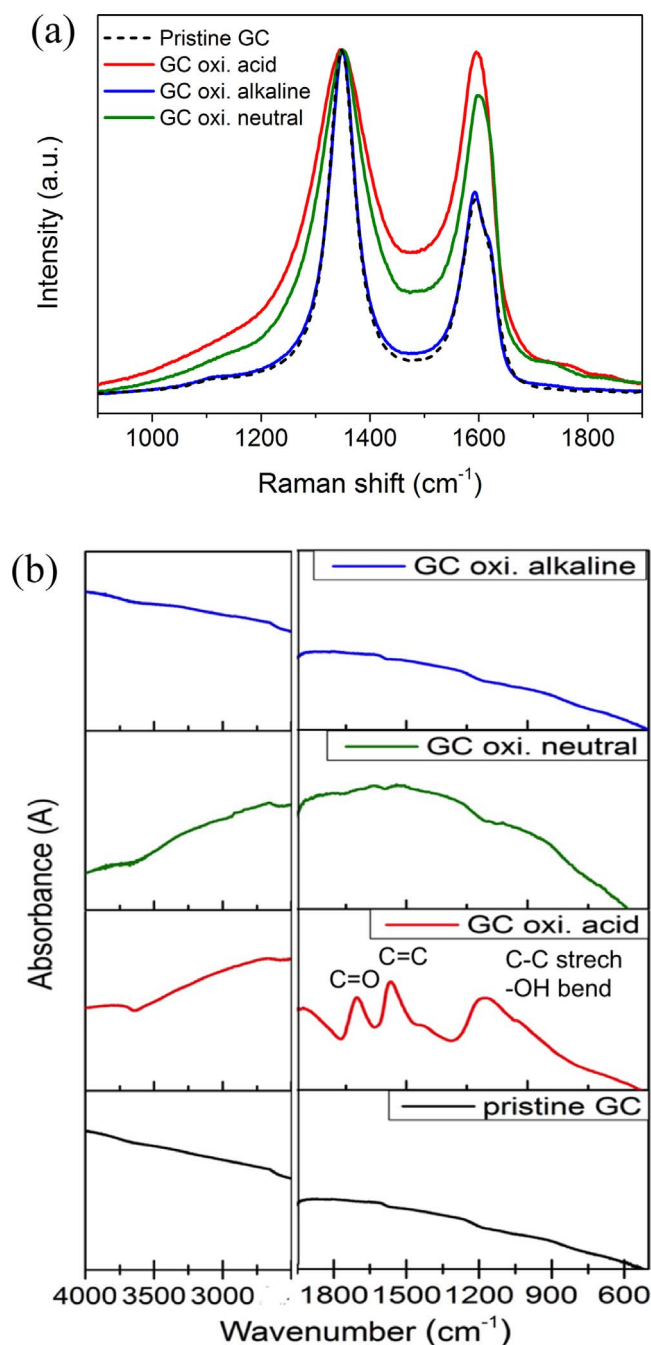


Fig. 5. Raman (a) and infrared (b) spectrum of pristine GC, GC oxidized in acidic, neutral and alkaline media.

the O1 s of pristine GC from the O1 s of the oxidized GC) undoubtedly support that the carbon oxidized in acidic media contains predominantly C–O groups, whereas the carbon oxidation in alkaline media creates mainly C=O groups, as shown in Fig. S8. Additionally, the increase of negative and positive charged molecules on the GC oxidized in alkaline media could be from carbonate ions or OH· radicals present in the media. These results give further evidence that different corrosion behavior of GC in acidic and alkaline media, are consistent with the results discussed above.

Our observations in this study clearly show the difference in electrochemical corrosion behavior of glassy carbon in acidic and alkaline media at an oxidative environment. The prolonged electrolysis on a carbon electrode at high anodic potential leads to the destruction of carbon surface due to carbon oxidation. At low pH, carbon is oxidized

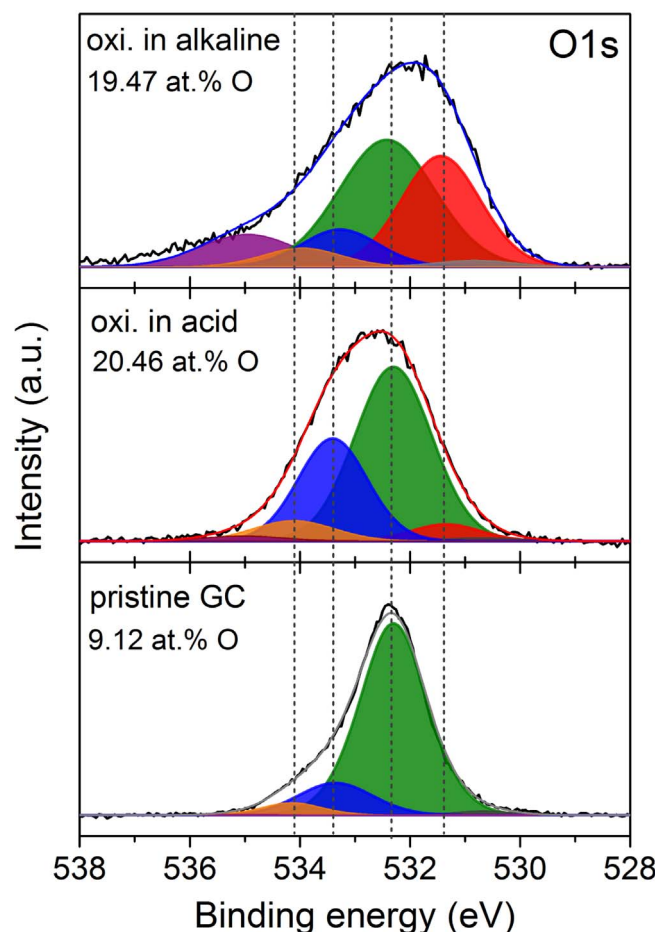


Fig. 6. O1s XPS of pristine GC, GC oxidized in acidic and alkaline media.

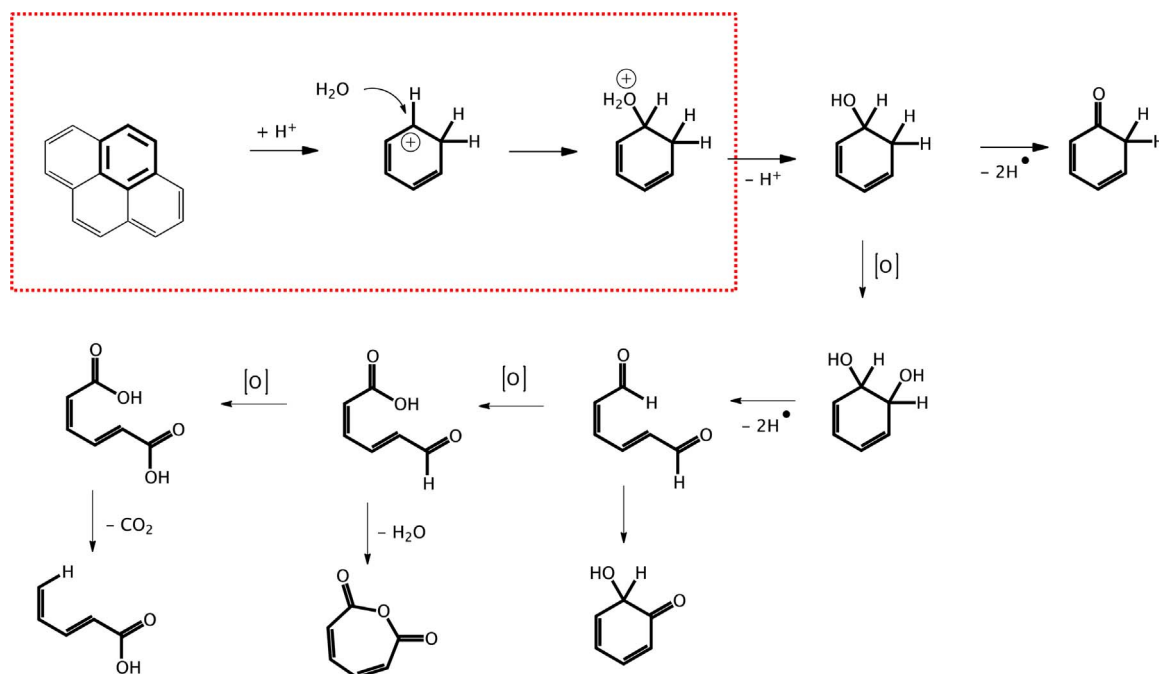
Table 2

The amount of functional groups obtained from the O1 s fitting of XPS analysis.

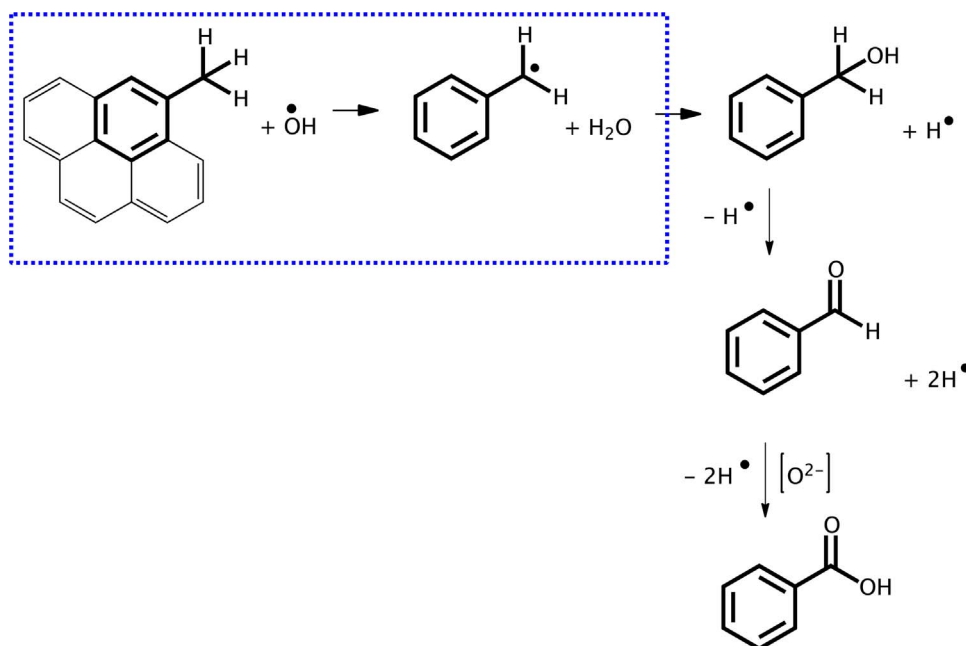
Peak [eV]	Pristine GC [%]	GC oxidized in acid [%]	GC oxidized in alkaline [%]
530.72 Negatively charged molecules, $\text{CO}_3^{2-}$	1.53	1.1	1.74
531.37 =O in carbonyls, lactone, anhydride, carboxyls	–	4.83	30.37
532.25 –O in $\text{H}_2\text{O}$ , hydrogen bridge bond	79.00	55.80	42.25
533.35 –O in hydroxyls, ether, lactone, carboxyls	14.43	29.57	9.93
534.16 –O in anhydride	4.62	6.94	5.09
534.88 Positively charged particles, graphite flakes	0.41	1.75	10.02

by forming surface oxides. It is evident from the result that the GC oxidized in acidic media contains the redox peak in cyclic voltammetry, the existence of an oxide layer in SEM, the evidence of functionalized carbon in Raman and infrared spectroscopy, and the contribution of C–O groups in XPS. On the other, at high pH, carbon is oxidized followed by dissolution. Although there is no drastic change of the GC oxidized in alkaline media in Raman and infrared spectroscopy, SEM images show noticeably a cracked holed surface caused by carbon dissolution. In addition, the break of a graphite structure by the oxidation in alkaline media can be supported by the existence of carbonyl group (C=O) and graphite flake on the GC oxidized in alkaline media from XPS.

The different degradation behavior of a carbon electrode depending



**Scheme 1.** Proposed acid catalyzed electrophilic reaction mechanism in acidic media (dotted box) and a few further possible oxidation steps to carboxylic groups, anhydrides, aldehydes or alcohols that lead to a ring deformation or opening based on the spectroscopic results.



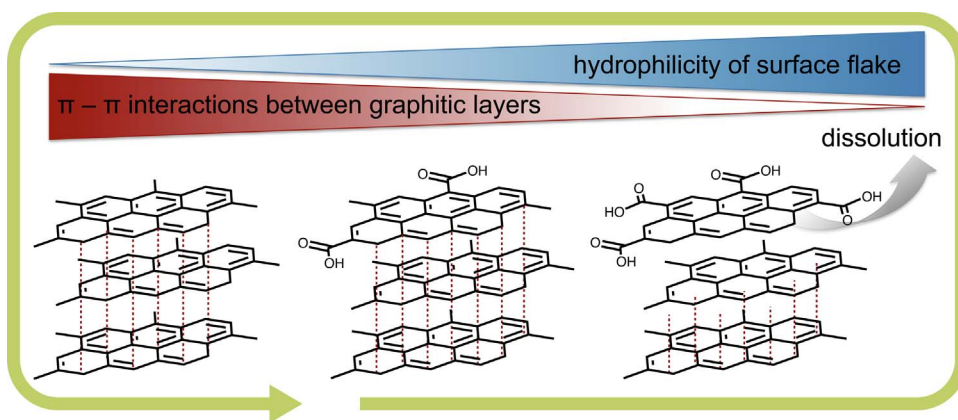
**Scheme 2.** Local selective radical substitution at alkyl site chains in alkaline media (dotted box) and possible ongoing oxidation based on the spectroscopic results.

on the pH of electrolyte could be explained by principal reactions of the electrochemical oxidation of carbon in acidic and alkaline aqueous electrolyte. We propose that in acidic media the presence of protons catalyze the electrophilic addition or substitution of water in a conjugated  $\pi$ -system. Subsequent supposed oxidation and condensation steps are based on known oxidation mechanism in organic chemistry (Scheme 1). In the scheme only a few organic pathways are suggested including oxidation steps with oxygen in nascent state from OER. Electrochemical oxidation pathways are not elaborated. The possible reaction pathways can lead to the formation of ketones, aldehydes and carboxylic groups, which is in accordance with XPS results. Electrophilic substitutions take place at aromatic system as they are present in the small graphitic entities of the glassy carbon electrode, therefore the oxidation of the glassy carbon can appear at defects at the GC surface as

seen by microscopy. For the reason that the experiments were performed in sulfuric acid,  $SO_3$  might be as well an electrophile that could react in an aromatic sulfonation reaction, which would explain the presence of sulfur in the EDX analysis. Due to the ring opening of the graphitic structures the acidic media can penetrate deeper in the electrode with proceeding electrocatalytic oxidation, accordingly the capacity increases after an initial oxidation of the surface linearly with the generated surface and proceeding oxidation of it. Correspondingly, bulk sensitive spectroscopic methods like Raman, IR and EDX are able to determine the formation of functional groups.

On the other hand, the oxidation procedure in alkaline media could be explained by a radical process. The reaction of  $OH^-$  ions at anodic potentials leads to the formation of hydroxyl radicals ( $OH^\bullet$ ) by discharge of  $OH^-$ . Radicals react preferentially with alkyl site chains as





**Scheme 3.** Proposed process during electrocatalytic oxidation processes of GC in alkaline media.

depicted in Scheme 2. Subsequently, these groups can be further oxidized over aldehydes to carboxylic acid groups and detected by surface sensitive XPS. Correspondingly the negatively charged molecules as well as the C=O amount increases more significant in the case of GC oxidation in alkaline media. Considering, that the radical reaction begins mainly at alkyl site chains and therefore at the edges of the small graphitic domains, the layer becomes more and more hydrophilic until the  $\pi$ - $\pi$  interaction between the flakes and the GC becomes weaker and dissolve in the electrolyte (Scheme 3). A raw GC surface would therefore remain. This supposed mechanism is in good agreement with the spectroscopic methods as only surface oxides are performed before the flakes dissolve. Additionally the kinetic interpretation of the chronoamperograms support the supposed reaction pathways since radical processes as supposed in alkaline media are faster than the acid catalyzed reaction in acidic media. Also the progress of the increase of the capacity and reaching of a plateau supports the assumed reaction mechanism since after a rapid initial oxidation the dissolution of the oxidized flakes leaves always a fresh GC surface behind. A clean surface of the GC after oxidation in alkaline media is also seen by microscopy.

#### 4. Summary

This paper has explored the degradation of a glassy carbon (GC) electrode by electrochemical oxidation at high anodic potentials, revealing that it is not inert under these conditions. Microscopic and spectroscopic analysis can identify the surface changes of GC caused by the oxidation. The electrochemical signature of the oxidation progress matches to the applied spectroscopic methods. Depending on the pH of electrolyte two different degradation mechanisms are supposed. On the one hand side carbon is oxidized by forming surface oxides at low pH supported by an acid catalyzed electrophilic reaction. Functional groups formed by the oxidation in acidic media were characterized by spectroscopic analysis corresponding to the change of the electrochemical capacitance. In alkaline media a radical mechanism is assumed to be responsible for the initiation of oxide formation. Predominantly the edges of small graphitic structures are oxidized as far as they become sufficiently hydrophilic and dissolve in the electrolyte. Although GC is chemically relatively stable compared to other types of carbon materials, its degradation caused by the electrochemical oxidation of carbon at anodic potential is inevitable. However, in spite of the instability of carbon electrodes at highly oxidizing conditions, carbon materials are still electrochemically competitive for a catalyst support compared to conducting metal oxides and are promising for metal-free electrocatalysts due to their high conductivity and low cost. Carbon materials applied at high anodic potentials, or GC used as a substrate for the investigation of coated catalysts for oxygen-involving reaction, can be influenced by these conditions, as shown with the reported results. The surface changes of the carbon electrode over time and the different oxidation mechanism in dependence of the media

should be kept in sight when carbon electrodes are applied, especially at high anodic potential involving both carbon and water oxidation.

#### Acknowledgements

The authors would like to thank Anna Mechler for scientific discussions and the Max Planck Society for funding.

#### Appendix A. Supplementary data

Supplementary data associated with this article can be found, in the online version, at <http://dx.doi.org/10.1016/j.cattod.2017.07.013>.

#### References

- [1] N. Alexeyeva, E. Shulga, V. Kisand, I. Kink, K. Tammeveski, Electroreduction of oxygen on nitrogen-doped carbon nanotube modified glassy carbon electrodes in acid and alkaline solutions, *J. Electroanal. Chem.* 648 (2010) 169–175.
- [2] J.Y. Cheon, T. Kim, Y. Choi, H.Y. Jeong, M.G. Kim, Y.J. Sa, J. Kim, Z. Lee, T.-H. Yang, K. Kwon, O. Terasaki, G.-G. Park, R.R. Adzic, S.H. Joo, Ordered mesoporous porphyrinic carbons with very high electrocatalytic activity for the oxygen reduction reaction, *Sci. Rep.* 3 (2013).
- [3] K. Gong, F. Du, Z. Xia, M. Durstock, L. Dai, Nitrogen-doped carbon nanotube arrays with high electrocatalytic activity for oxygen reduction, *Science* 323 (2009) 760–764.
- [4] W. He, C. Jiang, J. Wang, L. Lu, High-rate oxygen electroreduction over graphitic-N species exposed on 3D hierarchically porous nitrogen-doped carbons, *Angewandte Chemie* 53 (2014) 9503–9507.
- [5] H.B. Yang, J. Miao, S.F. Hung, J. Chen, H.B. Tao, X. Wang, L. Zhang, R. Chen, J. Gao, H.M. Chen, L. Dai, B. Liu, Identification of catalytic sites for oxygen reduction and oxygen evolution in N-doped graphene materials: development of highly efficient metal-free bifunctional electrocatalyst, *Sci. Adv.* 2 (2016) e1501122.
- [6] S. Chen, J. Duan, M. Jaroniec, S.Z. Qiao, Nitrogen and oxygen dual-doped carbon hydrogel film as a substrate-free electrode for highly efficient oxygen evolution reaction, *Adv. Mater.* 26 (2014) 2925–2930.
- [7] Y. Zhao, R. Nakamura, K. Kamiya, S. Nakanishi, K. Hashimoto, Nitrogen-doped carbon nanomaterials as non-metal electrocatalysts for water oxidation, *Nat. Commun.* 4 (2013).
- [8] N. Cheng, Q. Liu, J. Tian, Y. Xue, A.M. Asiri, H. Jiang, Y. He, X. Sun, Acidically oxidized carbon cloth: a novel metal-free oxygen evolution electrode with high catalytic activity, *Chem. Commun.* 51 (2015) 1616–1619.
- [9] X. Lu, W.L. Yim, B.H. Suryanto, C. Zhao, Electrocatalytic oxygen evolution at surface-oxidized multiwall carbon nanotubes, *J. Am. Chem. Soc.* 137 (2015) 2901–2907.
- [10] D. Guo, R. Shibuya, C. Akiba, S. Saji, T. Kondo, J. Nakamura, Active sites of nitrogen-doped carbon materials for oxygen reduction reaction clarified using model catalysts, *Science* 351 (2016) 361–365.
- [11] K. Kinoshita, *Carbon Electrochemical and Physicochemical Properties*, John Wiley & Sons, Inc., 1987.
- [12] F. Hasche, M. Oezaslan, P. Strasser, Activity, stability and degradation of multi walled carbon nanotube (MWCNT) supported Pt fuel cell electrocatalysts, *Phys. Chem. Chem. Phys.* 12 (2010) 15251–15258.
- [13] C.A. Reiser, L. Bregoli, T.W. Patterson, J.S. Yi, J.D. Yang, M.L. Perry, T.D. Jarvi, A reverse-current decay mechanism for fuel cells, *Electrochem. Solid State Lett.* 8 (2005) A273.
- [14] M. Carmo, D.L. Fritz, J. Mergel, D. Stolten, A comprehensive review on PEM water electrolysis, *Int. J. Hydrogen Energy* 38 (2013) 4901–4934.
- [15] H. Dau, C. Limberg, T. Reier, M. Risch, S. Roggan, P. Strasser, The mechanism of water oxidation: from electrolysis via homogeneous to biological catalysis,



- Chemcatchem 2 (2010) 724–761.
- [16] C. Xiang, K.M. Papadantonakis, N.S. Lewis, Principles and implementations of electrolysis systems for water splitting, *Mater. Horiz.* 3 (2016) 169–173.
- [17] Y. Yi, J. Tornow, E. Willinger, M.G. Willinger, C. Ranjan, R. Schlögl, Electrochemical degradation of multiwall carbon nanotubes at high anodic potential for oxygen evolution in acidic media, *ChemElectroChem* 2 (2015) 1929–1937.
- [18] P.J.F. Harris, New perspectives on the structure of graphitic carbons, *Crit. Rev. Solid State Mater. Sci.* 30 (2005) 235–253.
- [19] A.F. Craievich, On the structure of glassy carbon, *Mater. Res. Bull.* 11 (1976) 1249–1255.
- [20] G.M. Jenkins, K. Kawamura, Structure of glassy carbon, *Nature* 231 (1971) 175–176.
- [21] D.M. Anjo, M. Kahr, M.M. Khodabakhsh, S. Nowinski, M. Wanger, Electrochemical activation of carbon electrodes in base: minimization of dopamine adsorption and electrode capacitance, *Anal. Chem.* 61 (1989) 2603–2608.
- [22] P. Chen, R.L. McCreery, Control of electron transfer kinetics at glassy carbon electrodes by specific surface modification, *Anal. Chem.* 68 (1996) 3958–3965.
- [23] R.C. Engstrom, V.A. Strasser, Characterization of electrochemically pretreated glassy carbon electrodes, *Anal. Chem.* 56 (1984) 136–141.
- [24] M. Morita, R. Arizono, N. Yoshimoto, M. Egashira, On the electrochemical activation of alkali-treated soft carbon for advanced electrochemical capacitors, *J. Appl. Electrochem.* 44 (2013) 447–453.
- [25] A.I.B.F.G.K. Baucke, Z. Galus, G. Gritzner, G. Inzelt, K. Izutsu, H. Kahlert, T. Kakiuchi, V.V. Kharton, A. Kisiel, A. Lewenstam, K. Maksymiuk, A. Michalska, J. Migdalski, M. Rohwerder, F. Scholz, G.A. Snook, P. Spitzer, G. Tauber, E.V. Tsipis, G. Tsirlina, S. Wunderli, *Handbook of Reference Electrodes*, Springer, 2013.
- [26] L.J. Kopley, A.J. Bard, Ellipsometric, electrochemical, and elemental characterization of the surface phase produced on glassy carbon electrodes by electrochemical activation, *Anal. Chem.* 60 (1988) 1459–1467.
- [27] C. Barbero, R. Kotz, Electrochemical activation of glassy-carbon – spectroscopic ellipsometry of surface phase formation, *J. Electrochem. Soc.* 140 (1993) 1–6.
- [28] K. Kinoshita, J.A.S. Bett, Potentiodynamic analysis of surface oxides on carbon blacks, *Carbon* 11 (1973) 403–411.
- [29] M.R. Tarasevich, V.A. Bogdanovskaya, N.M. Zagudaeva, Redox reactions of quinones on carbon materials, *J. Electroanal. Chem. Interfacial Electrochem.* 223 (1987) 161–169.
- [30] A. Dekanski, J. Stevanović, R. Stevanović, B.Ž. Nikolić, V.M. Jovanović, Glassy carbon electrodes, *Carbon* 39 (2001) 1195–1205.
- [31] P.N. Ross, H. Sokol, The corrosion of carbon-black anodes in alkaline electrolyte .1. acetylene black and the effect of cobalt catalyzation, *J. Electrochem. Soc.* 131 (1984) 1742–1750.
- [32] D. Alliata, P. Haring, O. Haas, R. Kotz, H. Siegenthaler, In situ atomic force microscopy of electrochemically activated glassy carbon, *Electrochem. Solid State Lett.* 2 (1999) 33–35.
- [33] M.G. Sullivan, B. Schnyder, M. Bärtsch, D. Alliata, C. Barbero, R. Imhof, R. Kötz, Electrochemically modified glassy carbon for capacitor electrodes characterization of thick anodic layers by cyclic voltammetry differential electrochemical mass spectrometry, spectroscopic ellipsometry, X-Ray photoelectron spectroscopy, FTIR, and AFM, *J. Electrochem. Soc.* 147 (2000) 2636.
- [34] A.C. Ferrari, J. Robertson, Raman spectroscopy of amorphous, nanostructured, diamond-like carbon, and nanodiamond, *Philosophical transactions, Series A, Mathematical, Phys., Eng. Sci.* 362 (2004) 2477–2512.
- [35] A. Sadezky, H. Muckenhuber, H. Grothe, R. Niessner, U. Pöschl, Raman microspectroscopy of soot and related carbonaceous materials: spectral analysis and structural information, *Carbon* 43 (2005) 1731–1742.
- [36] A.C. Ferrari, J. Robertson, Interpretation of Raman spectra of disordered and amorphous carbon, *Phys. Rev. B* 61 (2000) 14095–14107.
- [37] D.G. McCulloch, S. Pawar, A. Hoffman, Structural investigation of xenon-ion-beam-irradiated glassy carbon, *Phys. Rev. B* 50 (1994) 5905–5917.
- [38] T. Jawhari, A. Roid, J. Casado, Raman spectroscopic characterization of some commercially available carbon black materials, *Carbon* 33 (1995) 1561–1565.
- [39] W.M. Prest, R.A. Mosher, Fourier transform IR spectroscopic characterization of the functional groups on carbon black, *Colloids Surf. Repogr. Technol.* 200 (1982) 225–247.
- [40] C. Moreno-Castilla, M.V. López-Ramón, F. Carrasco-Marín, Changes in surface chemistry of activated carbons by wet oxidation, *Carbon* 38 (2000) 1995–2001.
- [41] M. Seredych, D. Hulicova-Jurcakova, G.Q. Lu, T.J. Bandoz, Surface functional groups of carbons and the effects of their chemical character, density and accessibility to ions on electrochemical performance, *Carbon* 46 (2008) 1475–1488.
- [42] R. Blume, D. Rosenthal, J.-P. Tessonnier, H. Li, A. Knop-Gericke, R. Schlögl, Characterizing graphitic carbon with X-ray photoelectron spectroscopy: a step-by-step approach, *ChemCatChem* 7 (2015) 2871–2881.
- [43] E. Desimoni, G.I. Casella, A. Morone, A.M. Salvi, XPS determination of oxygen-containing functional groups on carbon-fibre surfaces and the cleaning of these surfaces, *Surf. Interface Anal.* 15 (1990) 627–634.
- [44] H. Li, Determination of Oxygen Functionality on Highly Oriented Pyrolytic Graphite (HOPG), Department of Biology, Chemistry and Pharmacy, Free university of Berlin, 2012.
- [45] F. Pariente, F. Tobalina, M. Darder, E. Lorenzo, H.D. Abruna, Electrodeposition of redox-active films of dihydroxybenzaldehydes and related analogs and their electrocatalytic activity toward NADH oxidation, *Anal. Chem.* 68 (1996) 3135–3142.
- [46] D. Nematollahi, S.M. Golabi, Electrochemical study of catechol and 4-methylcatechol in methanol. Application to the electro-organic synthesis of 4,5-dimethoxy- and 4-methoxy-5-methyl-o-benzoquinone, *J. Electroanal. Chem.* 405 (1996) 133–140.